Supporting Information

Nonlinear Transport Behaviors in Anti-aromatic Cyclo[n]carbon-based (n = 4k) Molecular Devices

Junnan Guo[1], Wenhui Fang[1], Jian Huang[1], Lishu Zhang[2], Weikang Wu[1†], and Hui Li[1]*

[1]Key Laboratory for Liquid-Solid Structural Evolution and Processing of Materials, Ministry of Education, Shandong University, Jinan 250061, China

[2]Peter Grünberg Institut (PGI-1) and Institute for Advanced Simulation (IAS-1), Forschungszentrum Jülich, Jülich 52428, Germany

[†]E-mail: weikang_wu@sdu.edu.cn

[*]E-mail: lihuilmy@hotmail.com

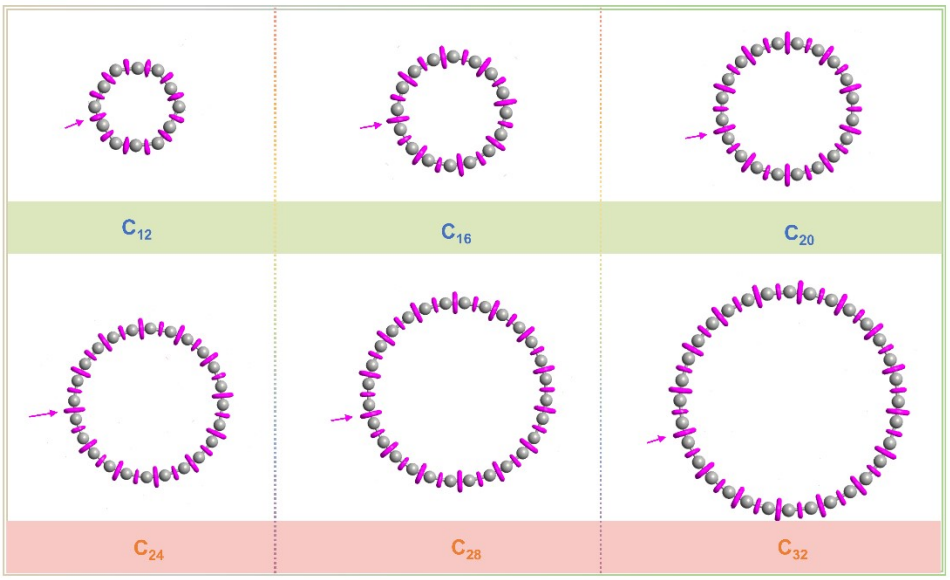

Figure S1. Electron localization function (ELF) (isovalue = 0.94 au) of C_n. Short C-C bonds in each map are highlighted by an arrow.

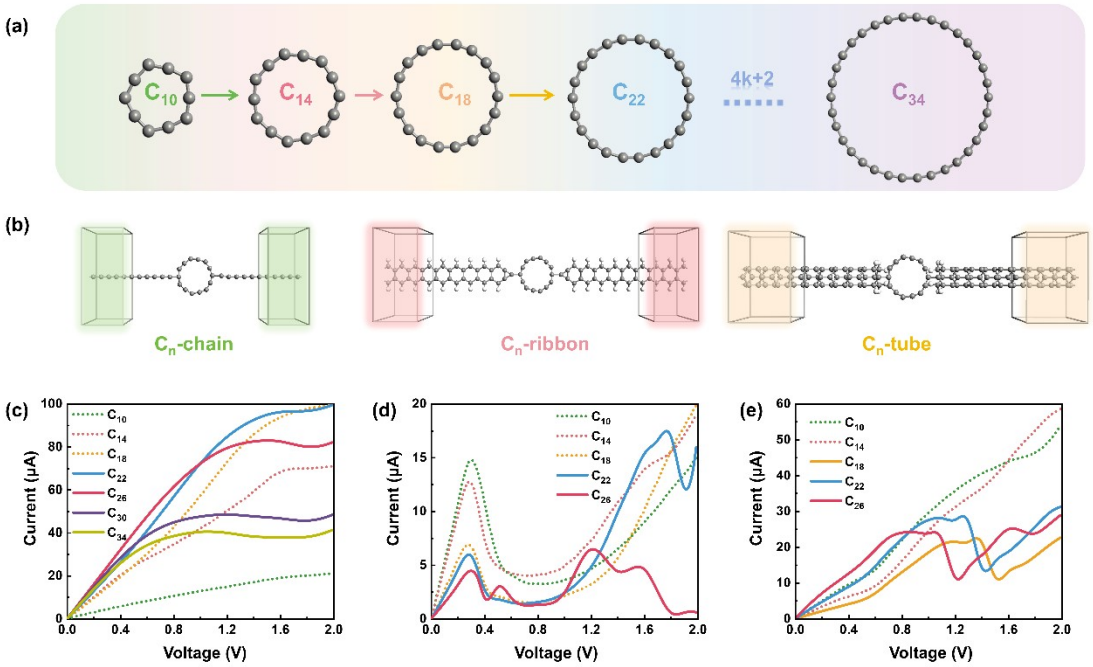

Figure S2. (a) Structures of C_n (n from 10 to 34). (b) Device configurations of C_n-chain , C_n-ribbon, and C_n-tube. I-V curves of C_n-chain (c), C_n-ribbon (d), and C_n-tube (e).

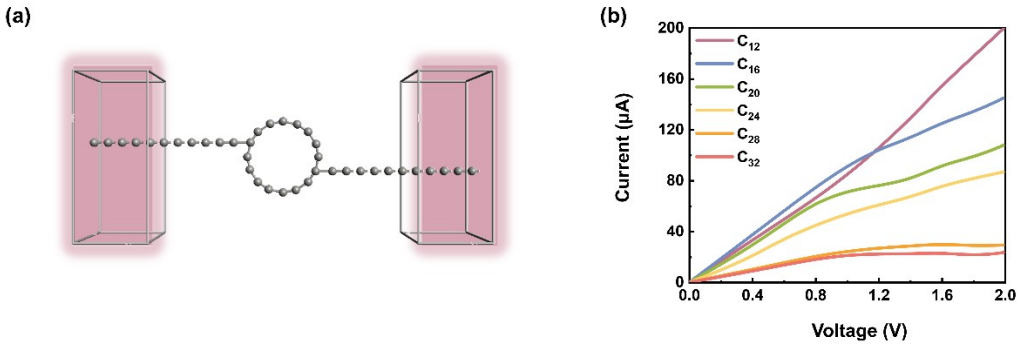

Figure S3. (a) Other device configurations of C_n-chain. (b) I-V curves of C_n-chain

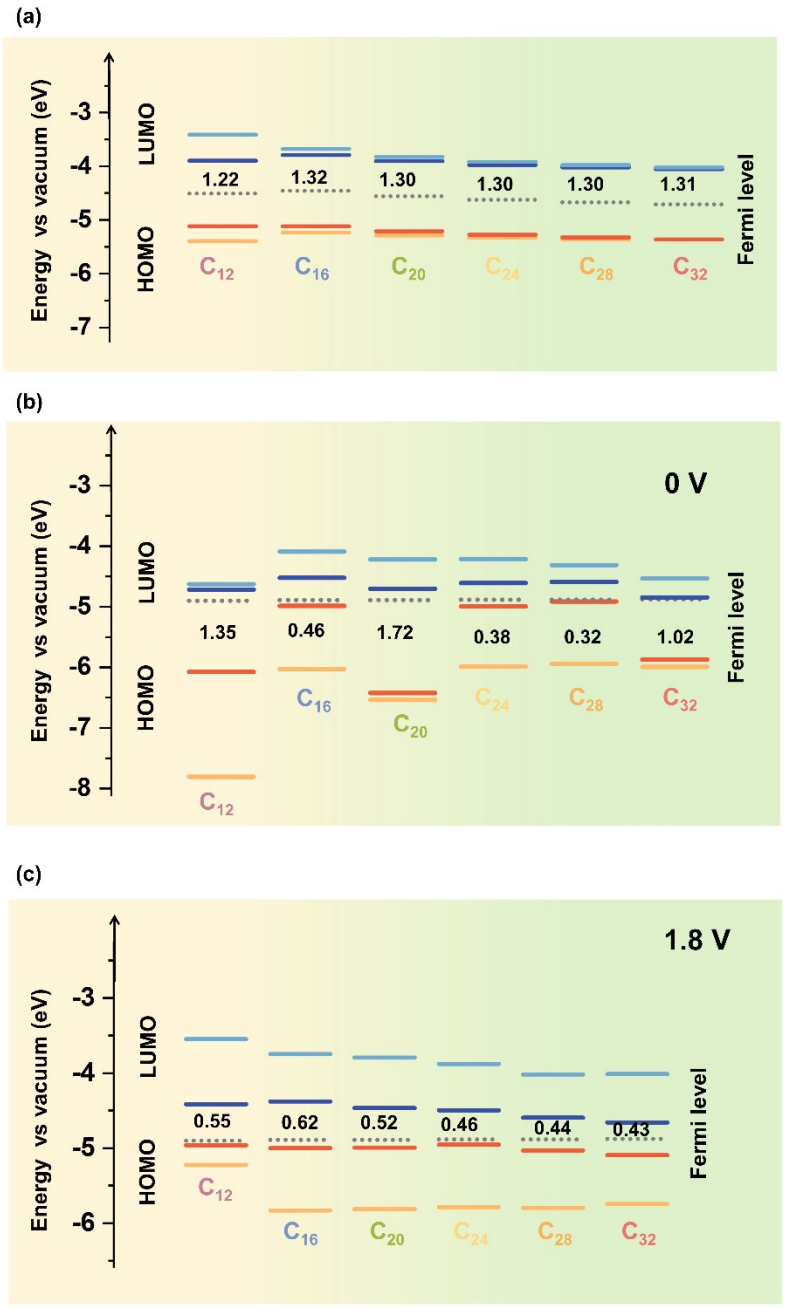

Figure S4. (a) Frontier molecular orbitals energies of C_n. (b) Frontier molecular orbitals energies of C_n at 0 V bias after device construction. (c) Frontier molecular orbitals energies of C_n at 1.8 V bias after device construction.

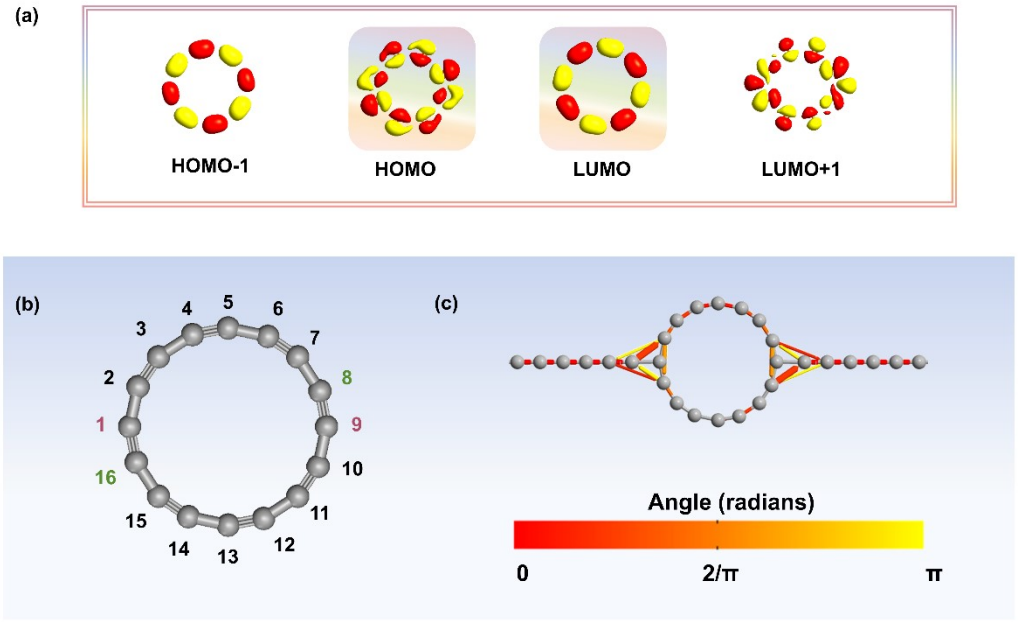

Figure S5. (a) Molecular projected self-consistent Hamiltonian quantities (MPSH) around the Fermi energy level of C_{16}-chain. (b) Numbers of atoms in C_{16} (c) Transmission pathways of C_{16}-chain.

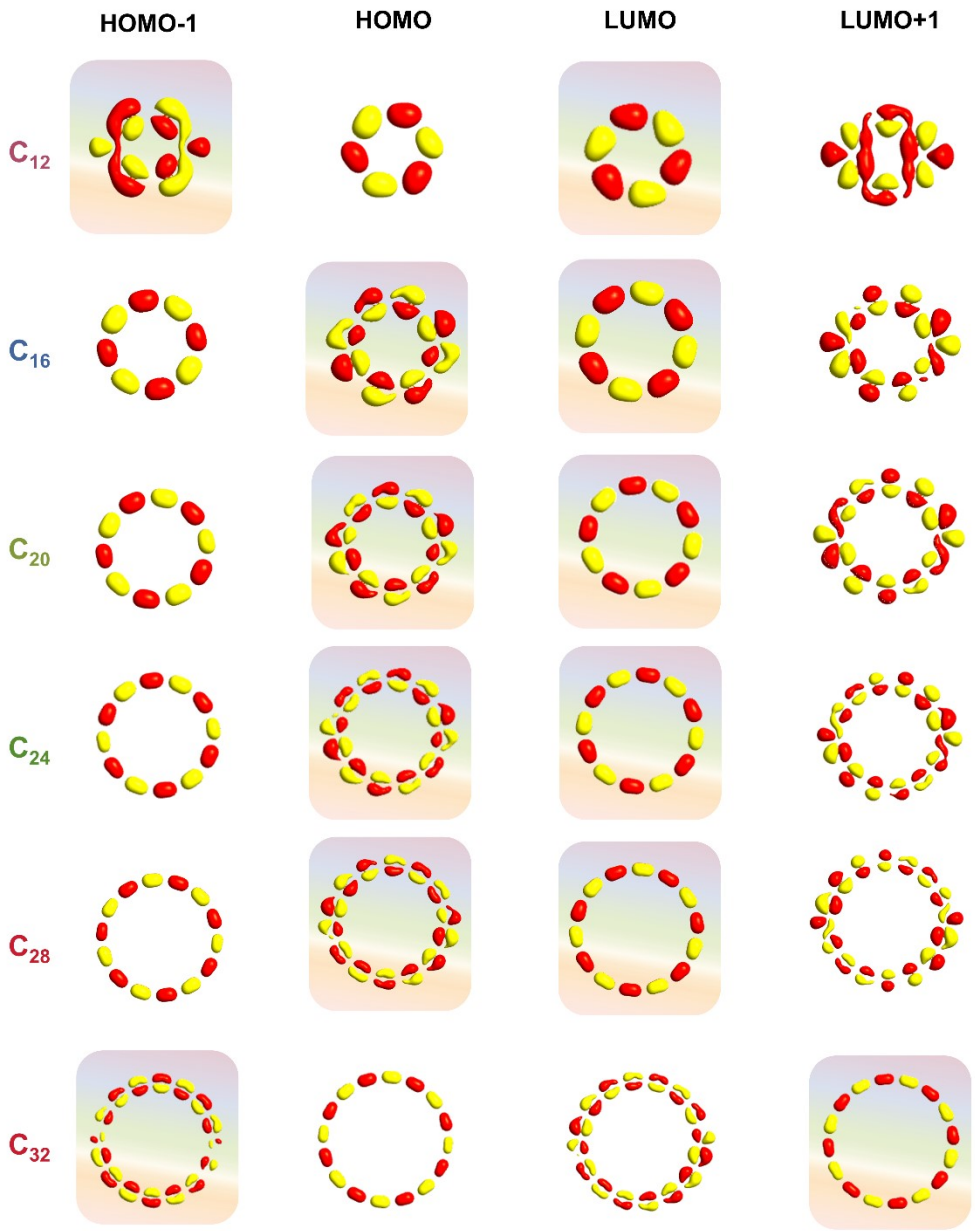

Figure S6. Molecular projected self-consistent Hamiltonian quantities (MPSH) around the Fermi energy level of C_n-chain. The dark shaded region is the dominant molecular orbital.

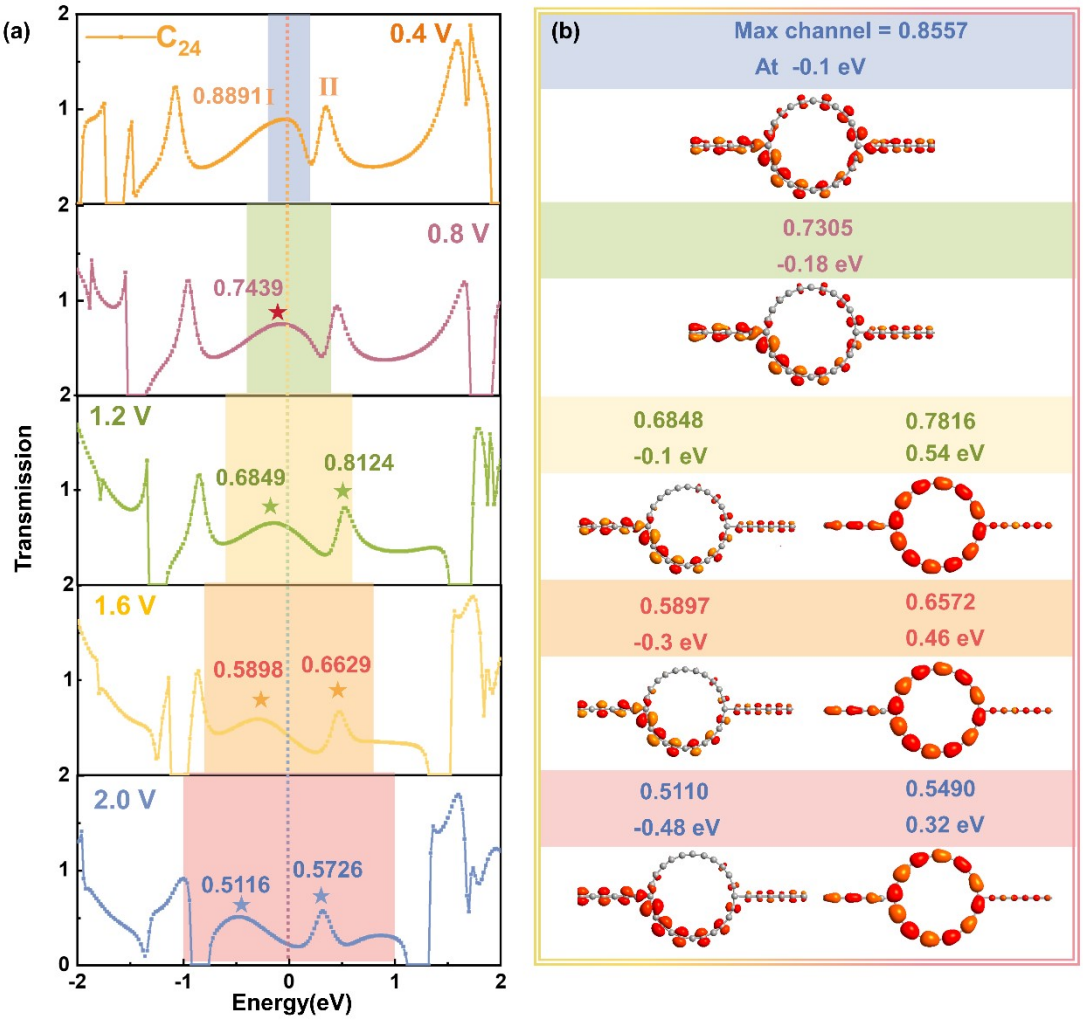

Figure S7. (a) Transmission spectra of device C_{24}-chain at typical biases. (b) Maximum transmission eigenvalues and transmission eigenstates of peaks I and II at corresponding biases.

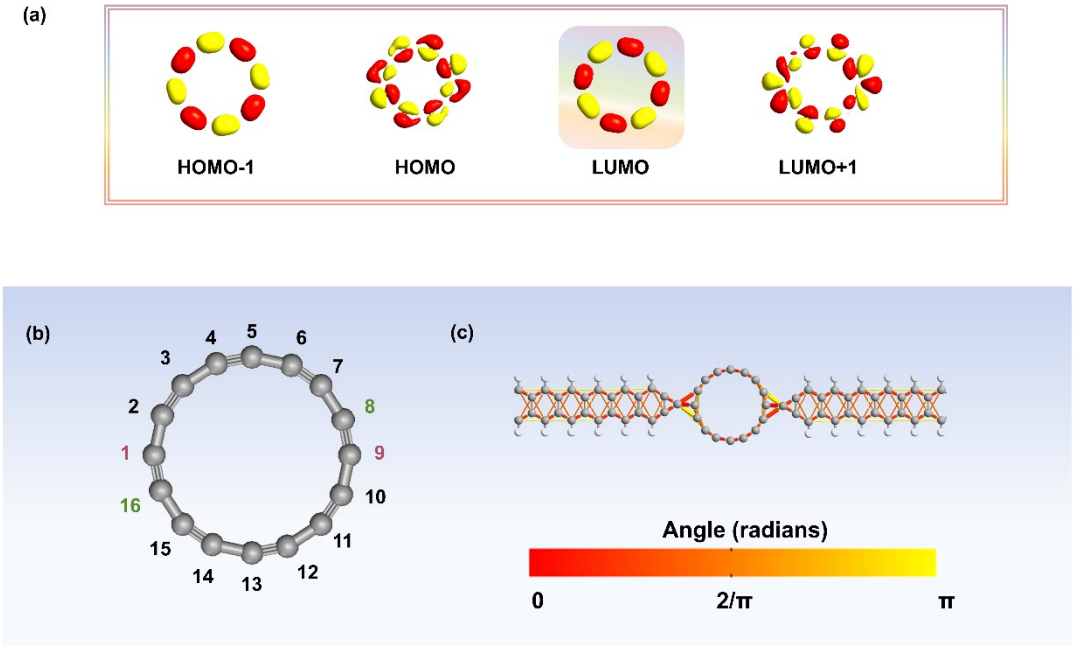

Figure S8. (a) Molecular projected self-consistent Hamiltonian quantities (MPSH) around the Fermi energy level of C_{16}-ribbon. (b) Numbers of atoms in C_{16}. (c) Transmission pathways of C_{16}-ribbon.

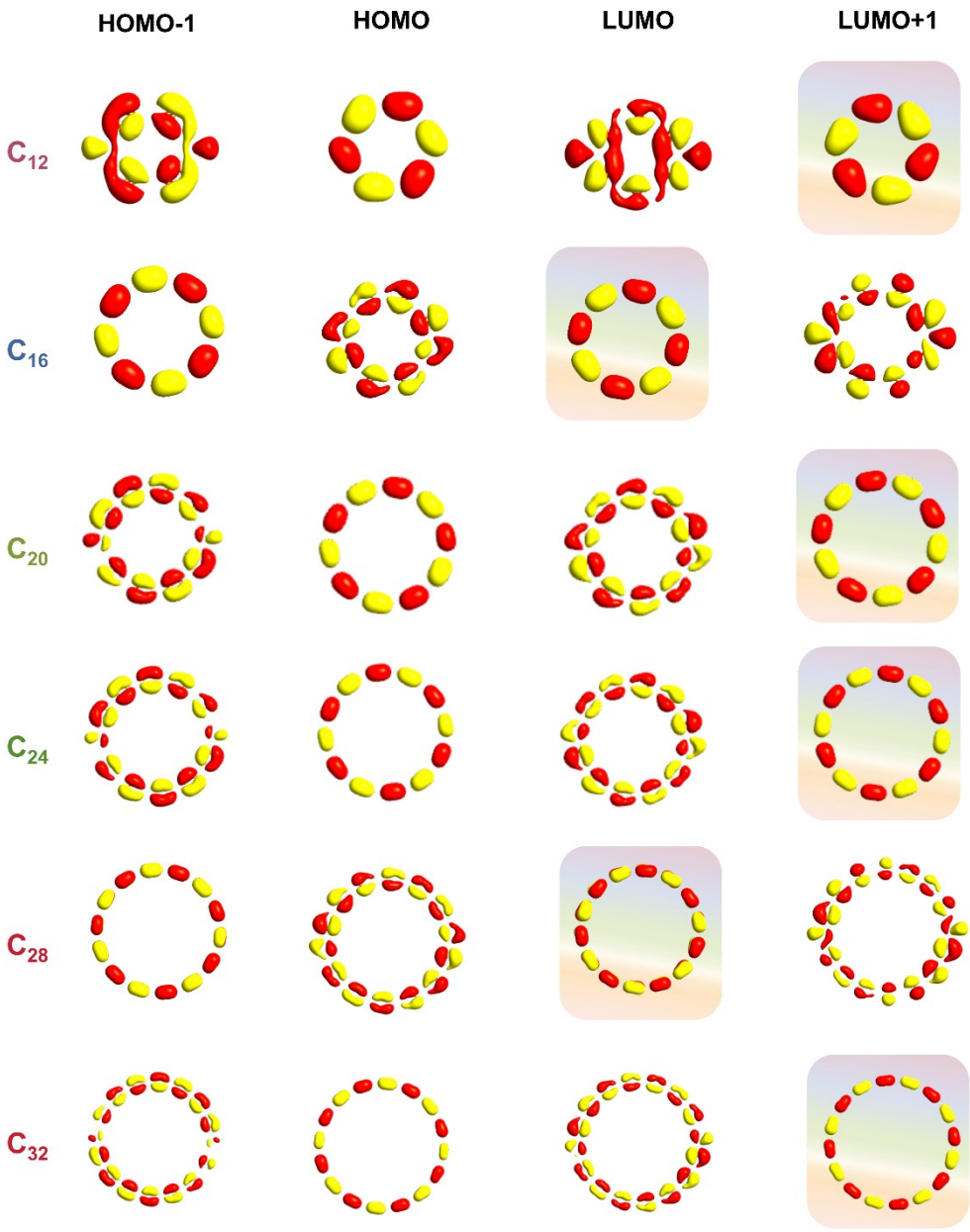

Figure S9. Molecular projected self-consistent Hamiltonian quantities (MPSH) around the Fermi energy level of C_n-ribbon. The dark shaded region is the dominant molecular orbital.

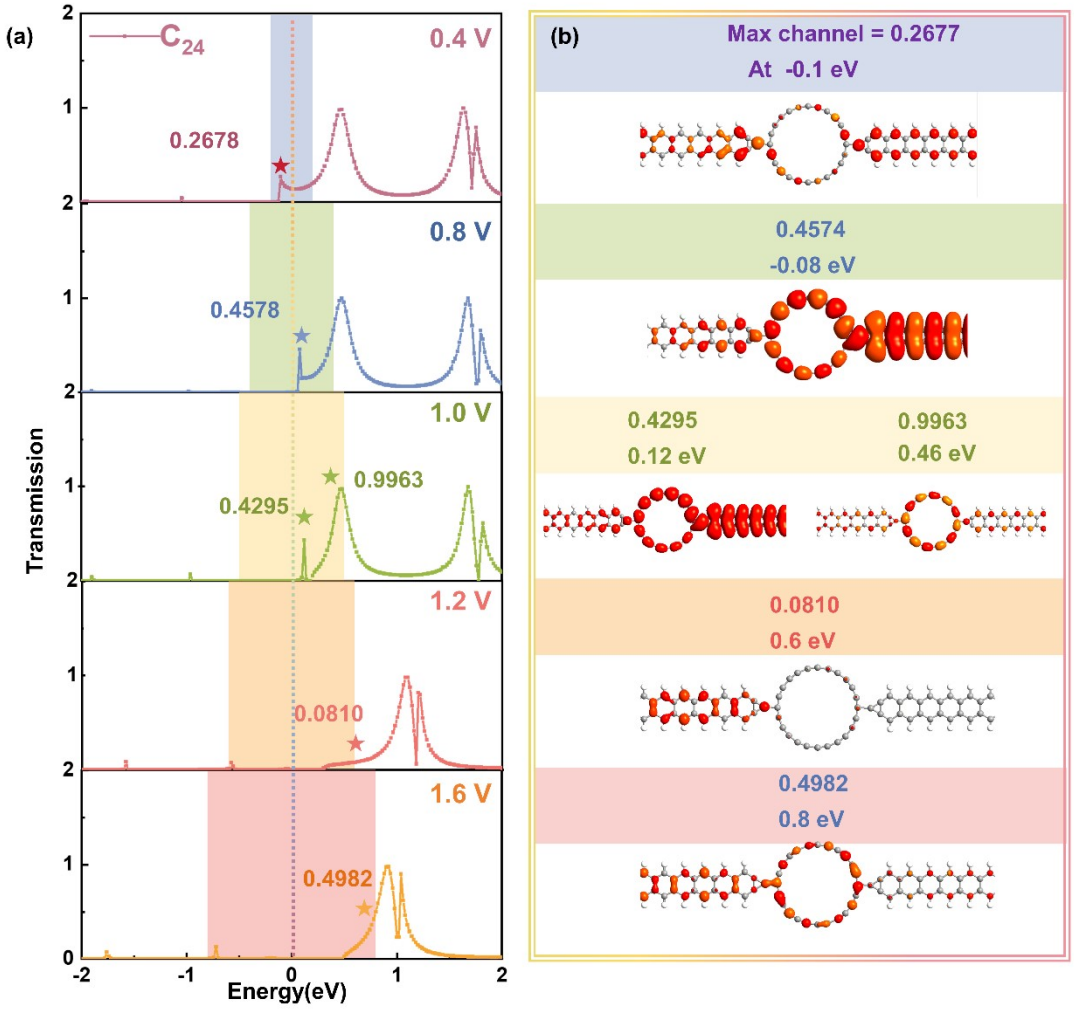

Figure S10. (a) Transmission spectra of device C_{24}-ribbon at typical biases. (b) Maximum transmission eigenvalues and transmission eigenstates of peaks I and II at corresponding biases.

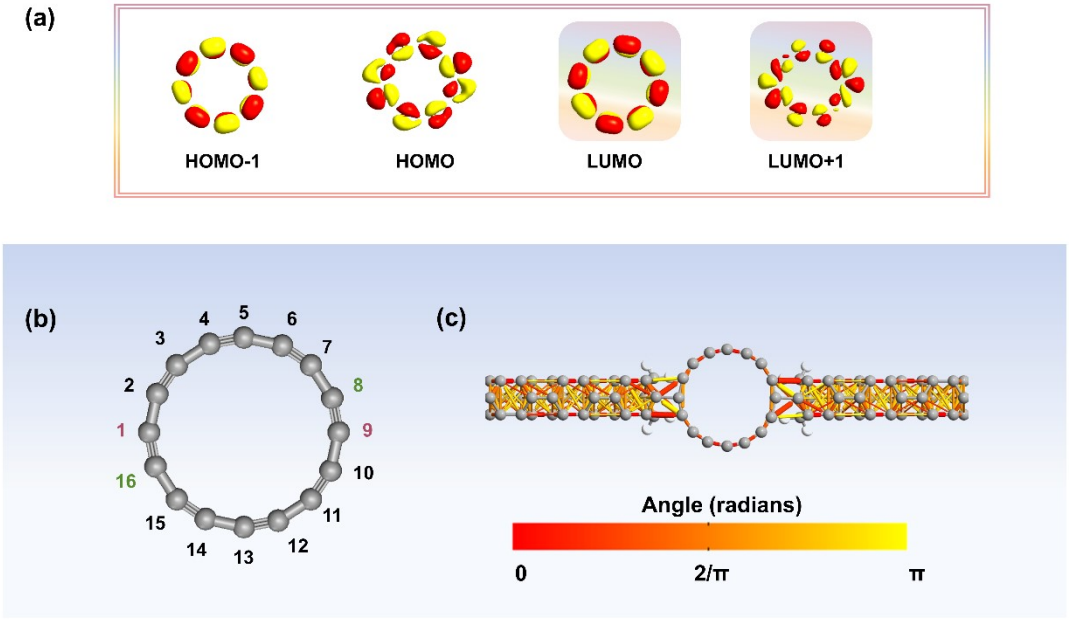

Figure S11. (a) Molecular projected self-consistent Hamiltonian quantities (MPSH) around the Fermi energy level of C_{16}-tube. (b) Numbers of atoms in C_{16}. (c) Transmission pathways of C_{16}-tube.

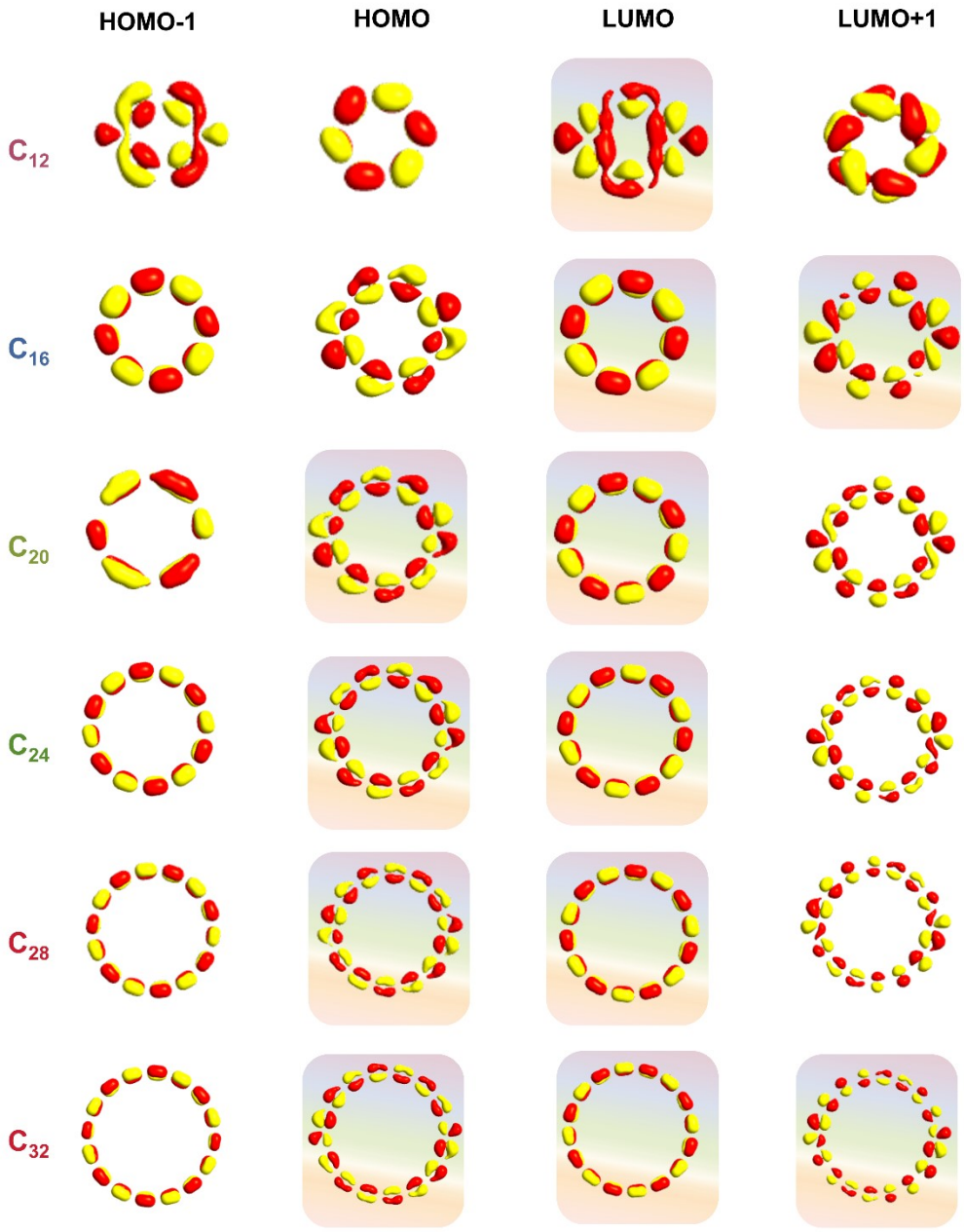

Figure S12. Molecular projected self-consistent Hamiltonian quantities (MPSH) around the Fermi energy level of C_n-tube. The dark shaded region is the dominant molecular orbital.

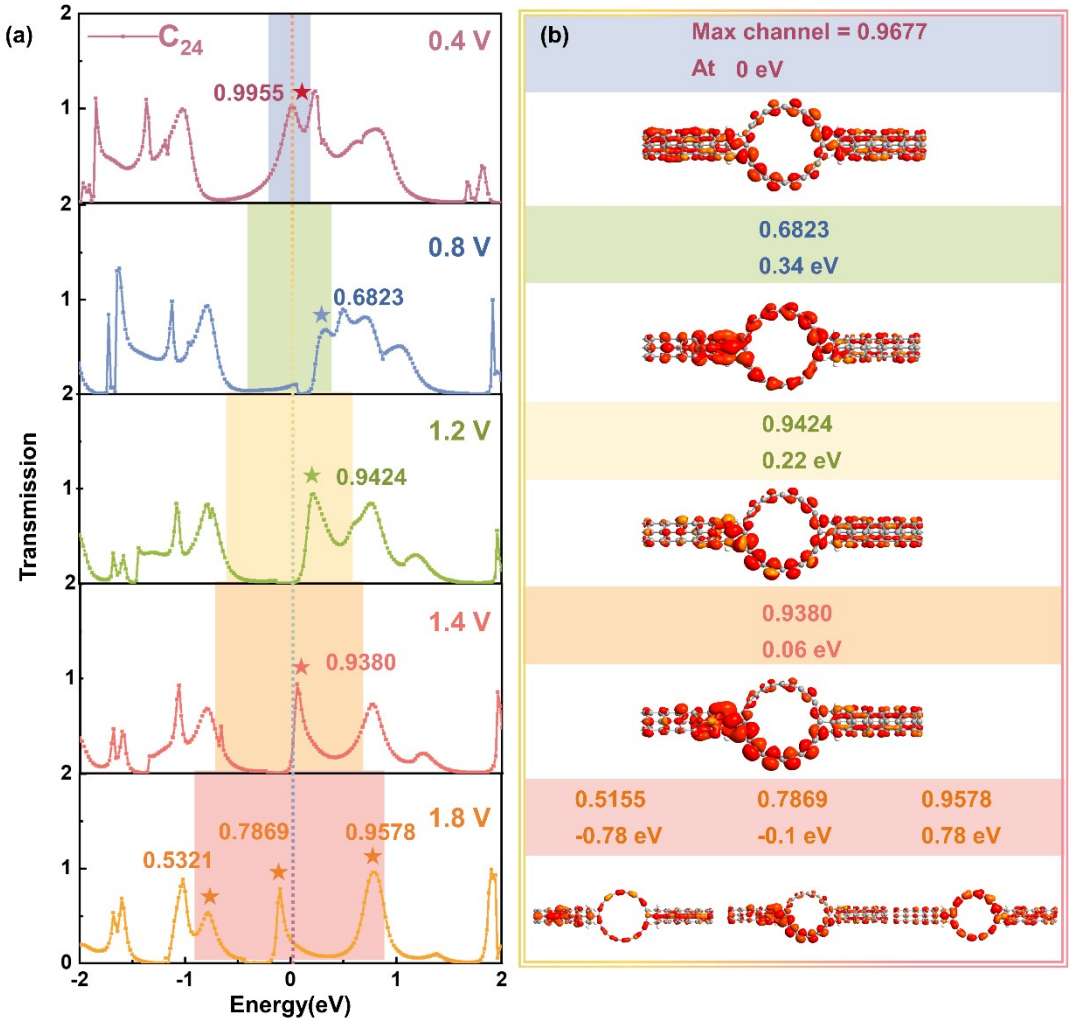

Figure S13. (a) Transmission spectra of device C_{24}-tube at typical biases. (b) Maximum transmission eigenvalues and transmission eigenstates of peaks I and II at corresponding biases.

Table S1. Performance comparison with other molecular-based devices

Molecule	Electrode	Bias voltage (V)	Current order of magnitude	I_{max}	Key characteristics	NDR Peak-to-Valley Ratio (PVR)
Cyclo[18]carbon[1]	carbon chain	[0, 1]	μA	~50	Ohmic characteristic	——
Cyclo[18]carbon[1]	graphene	[0, 1]	μA	~10	Quasi Schottky	——
Cyclo[18]carbon[1]	silver	[0, 1]	μA	~8	Current-limiting	——
Cyclo[14]carbon[2] (polyynic)	graphene	[0, 1]	μA	~15	NDR effect	~1.4
Cyclo[14]carbon[2] (cumulenic)	graphene	[0, 1]	μA	~20	Current-limiting	——
Trefoil knot[3] (24 benzenes)	silver	[0, 2]	nA	~80	NDR effect	~1.7
Cyclopropyllithium derivative[4]	carbon chain	[0, 3.5]	nA	~90	NDR effect	~6.1
Biphenyl[5]	gold	[0, 2]	μA	~10	NDR effect	~1.1
Phenylpyridine[5]	gold	[0, 2]	μA	~10	Nonlinearity	——
Thiophene Benzene-Based molecules[6]	graphene nanoribbon	[-2, 2]	μA	~20	Rectification; NDR effect	~3.0
Cyclo[n]carbon (Anti-aromatic)	carbon chain	[0, 2]	μA	~90	NDR effect; Current-limiting	~1.2
Cyclo[n]carbon (Anti-aromatic)	graphene nanoribbon	[0, 2]	μA	~25	NDR effect; Multi-NDR effect	~9.7
Cyclo[n]carbon (Anti-aromatic)	nanotube	[0, 2]	μA	~65	Multi-NDR effect; Oscillation	~1.9

References

1. L. Zhang, H. Li, Y. P. Feng and L. Shen, *J. Phys. Chem. Lett.*, 2020, **11**, 2611-2617.
2. Y. Liu, Z. Fang, B. Yao, J. Zhu, G. Tian and L. Ma, *Appl. Phys. Lett.*, 2025, **126**.
3. L. Zhu, Y. D. Guo, H. L. Zeng, H. X. Da, J. F. Li, Z. C. Liang, Y. Y. Jiang and X. H. Yan, *Phys. Lett. A*, 2021, **410**, 127539.
4. Y. D. Guo, P.-Y. Huang, X. X. Min, L.Y. Lin, M. Q. Rao, C. J. Dai, J. H. Li, P. Chen and X. H. Yan, *Phys. B: Condens. Matter*, 2022, **639**, 413989.

5. G. Berdiyorov and H. Hamoudi, *J. Mater. Res. Technol.*, 2021, **12**, 193-201.
6. Y. Xia, X. Zhang, C. Yuan, L. Zhang, X. Dai, T. Li, C. Fu and H. Li, *J. Phys. Chem. C*, 2019, **123**, 2766-2774.